RSC Advances

PAPER

View Article Online
View Journal | View Issue

Cite this: *RSC Adv.*, 2021, **11**, 26311

Template-assisted synthesis of Ag/AgCl hollow microcubes and their composition-dependent photocatalytic activity for the degradation of phenol†

Shiyun Lou, Qinglan Chen, Wan Wang, Yongqiang Wang and Shaomin Zhou *

Plasmonic photocatalysts with hollow structures and tunable composition exhibit significant advantages due to their high efficiency in light collection and effective charge transfer across the tight contact heterojunction interface. Herein, hollow Ag/AgCl microcubes were developed by treating nanosheet-assembled hollow Ag microcubes with $FeCl_3$, where a part of Ag at the interface could be *in situ* transformed and oxidized into AgCl. Equally, by adjusting the concentration of Fe^{3+} ions, Ag/AgCl hollow microcubes with different compositions could be easily achieved. Electron transfer was favored by a lot of tiny Ag/AgCl heterojunctions induced by the *in situ* oxidation of the multicrystalline Ag hollow microcube template containing a number of grain boundaries. The designed hollow Ag/AgCl microcubes exhibited strong visible-light adsorption owing to the surface plasmon resonance effect of Ag nanoparticles, in addition to the multiple light-reflections inside the hollow structure. The as-obtained products were then used as visible-light photocatalysts, where the results indicated that 91.6% of phenol was degraded within 150 min under visible light by the as-obtained sample with a Ag to AgCl ratio of 1 : 3. The superior visible-light photocatalytic activity resulted from the enhancement of the visible light-harvesting and the efficient charge separation at the Ag and AgCl contact interfaces.

Received 7th May 2021
Accepted 13th July 2021

DOI: 10.1039/d1ra03569j

rsc.li/rsc-advances

1. Introduction

Phenol in wastewater has posed a serious threat to the ecological environment and human health because of its high toxicity to human skin and harm to the central nervous system.[1] As a key protocol to remove phenol, photocatalysis has drawn extensive attention of researchers owing to its advantages of rapid decomposition, thorough treatment and no secondary pollution.[2,3] However, at present, photocatalysts still face problems such as low utilization efficiency of sunlight and short lifetime of photogenerated carriers, which limit their practical application. Therefore, it is of great significance to design and synthesize photocatalysts for efficient degradation of phenol pollutant in wastewater.

In recent years, plasmonic photocatalysts consisting of metallic nanoparticles and semiconducting components exhibit excellent photocatalytic performance owing to the integration of band structures of semiconductor materials, plasmonic properties of noble metals and generation of hetero interfaces.[4–6] For example, Ag/TiO_2 nanofibers[7] and Ag core–TiO_2 shell (Ag@TiO_2) nanoparticles[8] were found to be effective in photocatalytic degradation of phenol. However, interfaces between Ag and TiO_2 photocatalysts are not yet well controlled, resulting in uncertainties to improve the efficiency of charge separation at the interface between TiO_2 and Ag nanoparticles. Alternatively, a clean and well-defined Ag/AgCl interface can be achieved by *in situ* synthesis reaction.[9,10] It was demonstrated that hot electrons generated by Ag could inject into AgCl in 150 femtoseconds due to the excellent interface, which resulted in a significant improvement in the photocatalytic activity and stability of Ag/AgCl.[11–13]

It is well known that hollow structures are believed to further improve the catalytic performance of plasmonic photocatalysts thanks to the accessible surface and interior cavity, efficient light collection, shortened distance for carrier transfer and separation, rich surface reaction sites on the shells, and a uniform distribution of metal nanoparticles.[14–16] Furthermore, hollow semiconductors are lighter than the corresponding solid structure, and benefit the homogeneous dispersion in the reaction system of photocatalysis. As for hollow plasmonic photocatalysts, the powerful surface plasmonic resonance absorption and intracavity multiple reflections of visible light can improve the total absorption efficiency of photon energies.[17]

To date, the methods based on templates have been extensively applied in the preparation of hollow nanostructures, and

Key Laboratory for Special Functional Materials of the Ministry of Education, Henan University, Kaifeng 475004, PR China. E-mail: shaominzhou@yahoo.com; Tel: +86 371 22357375

† Electronic supplementary information (ESI) available. See DOI: 10.1039/d1ra03569j

the shape and size of cavities in the obtained hollow structures can be controlled by the designed templates.[18] Recently, hollow Ag/AgCl photocatalysts with hollow structures have been prepared and showed superior photocatalytic performance.[11,19,20] For example, Ag@AgCl cubic cages were obtained by the sacrificial template method, and exhibited great photocatalytic activity because of their hollow structures.[11] Ag@AgCl hollow spheres were synthesized by a chemical reduction approach under light irradiation, where $AgNO_3$ and CCl_4 were used as silver and chlorine sources, respectively.[19] Hollow cubic AgCl nanostructures were prepared by a one-pot method.[20] Thus, recently, most synthesis approaches for Ag/AgCl have been performed through the reduction process. Firstly, AgCl is prepared and then partly transformed to Ag by chemical reduction or photoreduction. Although this method is efficient for the preparation of hollow structure Ag/AgCl, the distribution of hetero interfaces between Ag and AgCl in the shell and the Ag/AgCl ratio are hard to manipulate; meanwhile, the amount and distribution of noble metals in plasmonic photocatalysts have an important influence on the photocatalytic performance.[21,22] In fact, an oxidation method was proposed to prepare Ag/AgBr nanowires, which is a simple experimental method, easy to operate, and the molar ratio of Ag to AgBr can be easily adjusted by controlling the concentration of the oxidizing agent composed of halide.[23] Furthermore, the *in situ* oxidation of Ag can form a close connection between Ag and AgBr and it is conducive to effective carrier transfer. In addition, solid Cu_2O/Ag/AgCl microcubes were synthesized by a facile oxidation method using Cu_2O/Ag microcubes as a template and $CuCl_2$ as an oxidant.[24] However, as far as we know, the controllable preparation of hollow Ag/AgCl microcubes by this oxidation method is rarely reported.

In this work, hollow Ag/AgCl microcubes with different compositions were synthesized through an *in situ* oxidization route. In the designed process, nanosheet-assembled hollow Ag microcubes were prepared as the template, and Ag/AgCl microcubes were obtained by employing $FeCl_3$ as the oxidizer at room temperature. The composition and structure of Ag/AgCl can be adjusted by rationally regulating the experimental conditions. Although AgCl with a hollow nanostructure has been synthesized, this report is the first on hollow Ag/AgCl microcubes synthesized using a nanosheet-assembled multicrystalline Ag microcube template to form a tight contact interface between Ag and AgCl, which is beneficial to the separation of photogenerated carriers. Furthermore, the obtained Ag/AgCl hollow microcubes show outstanding photocatalytic performance for the degradation of phenol.

2. Experimental details

2.1 Materials

Copper acetate ($Cu_2(CH_3COO)_2$), sodium hydroxide (NaOH), glucose ($C_6H_{12}O_6$), nitric acid (HNO_3), trisodium citrate (TSC, $C_6H_5Na_3O_7$), silver nitrate ($AgNO_3$), polyvinyl pyrrolidone (PVP), ferric chloride ($FeCl_3$), P25-TiO_2, methanol, ethanol and phenol were all purchased from Sinopharm Chemical Reagent Co., Ltd. All chemicals are of analytical reagent grade and need not to be further purified.

2.2 Synthesis of Ag/AgCl hollow microcubes

Firstly, uniform Ag hollow microcubes composed of nanosheets were prepared at room temperature using Cu_2O microcubes as the template according to the earlier literature of our group.[25] The synthesis of uniform Cu_2O microcubes was as follows: copper acetate (0.998 g) was dissolved in distilled water (100 mL). After the obtained solution was heated to 70 °C, NaOH solution (5 mL, 0.03 M) and glucose (0.2 g) were added successively under stirring. The mixture was maintained at 70 °C for 60 min. The precipitate was filtered and washed several times with deionized water and ethanol. The prepared Cu_2O was used as the template to synthesize Ag hollow microcubes. In a typical synthesis, Cu_2O (0.042 g) and trisodium citrate (0.176 g) were dispersed in distilled water (50 mL), and then $AgNO_3$ (0.204 g) was added. After 15 min, dilute HNO_3 (10 mL) was quickly injected into the vigorously stirred mixture. The color of the solution changed gradually from brick-red to grey, indicating the formation of silver microcubes. The reaction mixture was stirred for another 30 min after completing the reaction. The precipitate was separated by centrifugation, washed with deionized water and ethanol repeatedly, and dried at 60 °C for 4 h in a vacuum oven. Then, the as-synthesized Ag hollow microcubes and PVP (0.6 g) were dissolved into deionized water (10 mL). Finally, different concentrations of $FeCl_3$ solution (5 mL) were added to the solution containing Ag nanosheets and PVP drop by drop under continuous stirring. The AgCl nanoparticles were *in situ* formed on the Ag nanosheet surface by the oxidation of Ag and $FeCl_3$, where $FeCl_3$ was selected not only as the Cl^- source but also as the oxidizing agent. The solution mixture was magnetically stirred for 30 min to ensure a complete reaction. Using this approach, Ag/AgCl samples with various molar ratios were equally synthesized. The collected Ag/AgCl microcubes were rinsed four times with deionized water and centrifuged at 5000 rpm to get rid of unwanted $FeCl_3$ and PVP. In addition, nitrogen doped TiO_2 (N-TiO_2) and P25-TiO_2/Ag were used as photocatalysts in a controlled test. N-TiO_2 was synthesized by calcining P25-TiO_2 at 600 °C for 4 h in NH_3. P25-TiO_2/Ag was prepared according to the literature:[26,27] P25-TiO_2 powder (100 mg) was taken in different test tubes containing 120 mL water and 30 mL methanol, along with a certain amount of $AgNO_3$ solution (0.01 mM) and Ag–TiO_2 were purged with argon for 30 min and irradiated with a 400 W UV lamp under constant magnetic stirring for 2 h. The obtained solutions were centrifuged and washed with deionized water followed by ethanol. The resulting suspensions were separately dried in an oven at 60 °C for 12 h.

2.3 Characterization

The crystal phase of the as-obtained products was characterized by X-ray diffraction (XRD) with a powder XRD system (D8-ADVANCE, Bruker, Germany) using Cu Kα radiation (λ = 1.54056 Å). The morphology of Ag/AgCl microcubes was observed using a field-emission scanning electron microscope

(FESEM, Nova NanoSEM 450, FEI, USA). The compositions of the products were investigated using an energy-dispersive X-ray spectrometer (EDS) attached to the FESEM instrument. UV-Vis absorption spectra were recorded using a Cary 5000 UV-Vis spectrophotometer. X-ray photoelectronic spectroscopy (XPS) tests were carried out on an X-ray photoelectron spectrometer (XPS, AXIS ULTRA) and the binding energy of the spectrum was corrected by the reference of the C 1s peak (284.6 eV).

2.4 Photodegradation experiments

The photocatalytic performance of the as-synthesized Ag/AgCl hollow microcubes was evaluated by the phenol degradation experiments because phenol is a colorless, non-volatile and acute toxic organic pollutant in industrial waste water.[28,29] 160 mg photocatalysts were suspended in phenol (120 mL, 10 mg L^{-1}) aqueous solution. To achieve the absorption equilibrium, the obtained suspension was stirred for 30 min in the dark before irradiation. The light source was a solar simulator (xenon lamp 500 W) equipped with a cutoff filter (400 nm). During the process of photocatalytic reaction the suspensions (2.0 mL) were taken out at specific irradiation intervals, with removal of the photocatalyst by centrifugation. A Varian high-performance liquid chromatography (HPLC) system was equipped with an ultraviolet detector and it was adjusted at 269 nm to analyze the concentration of phenol. The mobile phase in a C18-reverse phase column was acetonitrile (70%)–water (29.5%)–phosphoric acid (0.5%) and the flow rate was 0.4 mL min^{-1}.

3. Results and discussion

3.1 Morphology and structure characterization

Fig. 1a shows that Ag hollow microcubes assembled by nanosheets were successfully prepared. The Ag microcubes were uniform with an average length of about 1.3 μm, and the microcubes presented a relatively rough surface and an internal hollow structure (Fig. 1b and c). Uniform Ag hollow microcubes were selected as the chemical template and reacted with $FeCl_3$. After reaction, the morphologies of the obtained samples were characterized by FESEM. In Fig. 1d, the morphology of the Ag/AgCl product still maintained a uniform microcube structure

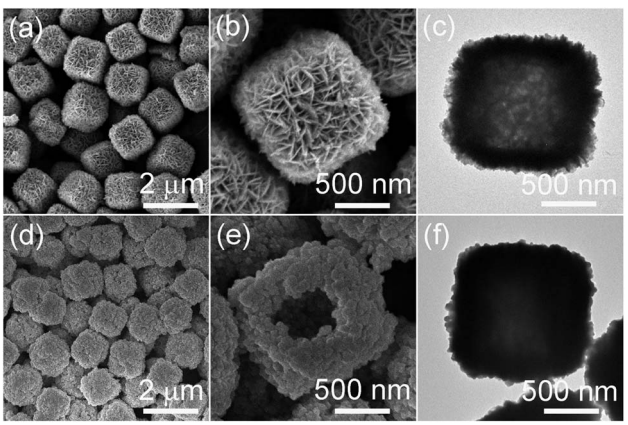

Fig. 1 Typical FESEM (a, b, d and e) and TEM (c and f) images of hollow Ag microcubes (a–c) and Ag/AgCl microcubes (d–f).

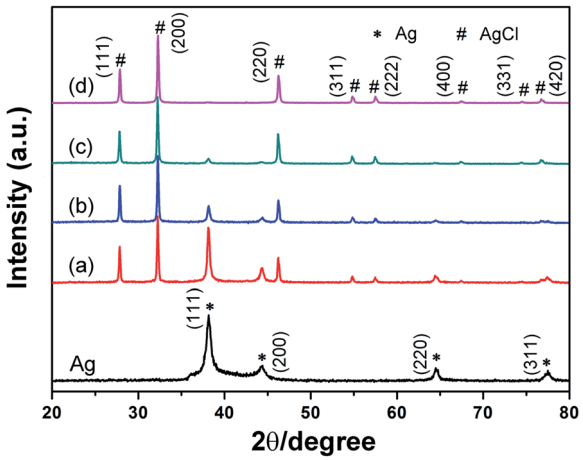

Fig. 2 XRD patterns of Ag and Ag/AgCl microcubes with various compositions (Ag : AgCl, (a) 3 : 1, (b) 1 : 1, (c) 1 : 3, and (d) 0 : 1).

and had a similar size to the Ag microcube template, which suggested that AgCl nanoparticles were instantly formed on the Ag microcubes. Even though Ag/AgCl microcubes maintained the hollow structure, the surface of Ag/AgCl microcubes changed from nanosheets to nanoparticles with an average size of tens of nanometers because the polycrystalline nanosheets on the surface of original Ag hollow microcubes were composed of Ag nanoparticles.

The XRD profiles of Ag and Ag/AgCl hollow microcubes with various component ratios are shown in Fig. 2. All the peaks of Ag hollow microcubes revealed that Ag was a cubic structure (JCPDS no. 04-0783). From XRD data, it could be seen that as $FeCl_3$ content increased, the XRD peak intensity of Ag slightly decreased until it completely vanished, and that of cubic-structure AgCl (JCPDS no. 31-1238) increased correspondingly. This indicated that Ag/AgCl hollow microcubes with various component proportions can be synthesized by adjusting the quantity of $FeCl_3$.

To investigate the influence of $FeCl_3$ concentration on the morphology of Ag/AgCl hollow microcubes, Ag/AgCl hollow microcubes with different compositions were further studied by FESEM. As shown in Fig. 3, with the increasing ratio of $FeCl_3$ to Ag, the particles on the surface of Ag/AgCl microcubes become

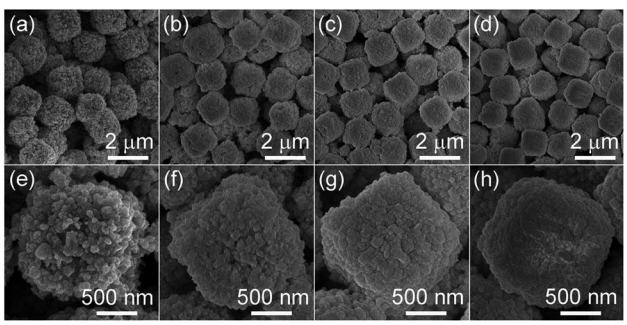

Fig. 3 FESEM images (a–d) of Ag/AgCl microcubes with various compositions (Ag : AgCl, (a) 3 : 1, (b) 1 : 1, (c) 1 : 3, and (d) 0 : 1), and their corresponding magnified images (e), (f), (g) and (h), respectively.

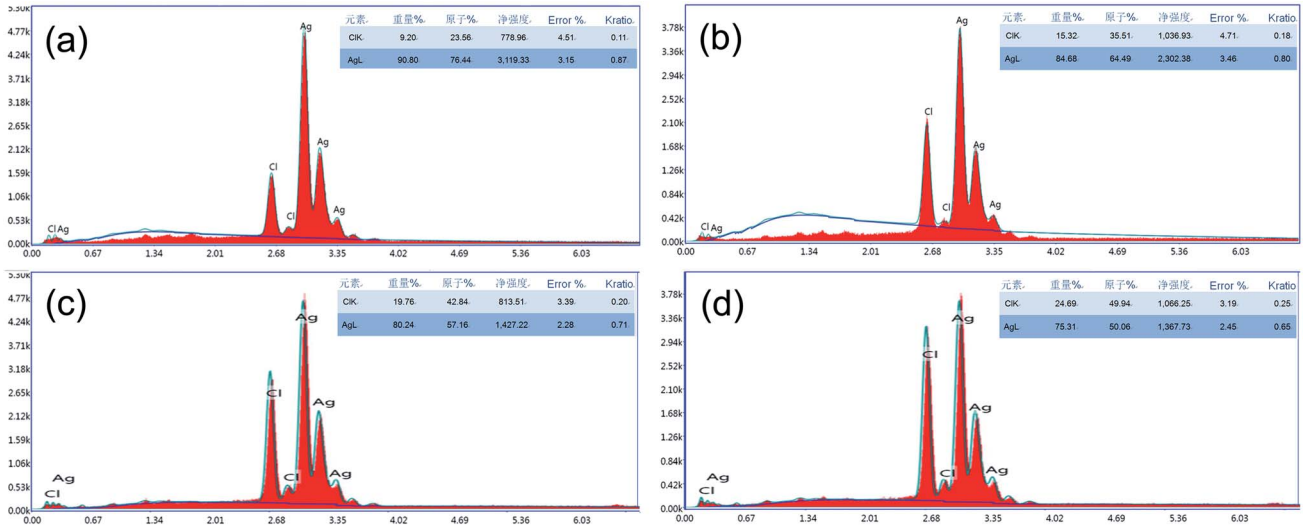

Fig. 4 EDS spectra of Ag/AgCl microcubes with various compositions (Ag : AgCl, (a) 3 : 1, (b) 1 : 1, (c) 1 : 3, and (d) 0 : 1).

denser gradually. The mean size of Ag/AgCl hollow microcubes was about 1.3 μm, indicating that the obtained Ag/AgCl products copied the original hollow Ag microcube template. Though the magnified images show that the final products consisted of nanoparticles, the packing density was significantly different. In Fig. 3e–h, when the ratio of Ag to AgCl was higher than 1 : 1, the surface of Ag/AgCl microcubes with a large number of pores was composed of loose nanoparticles, but when the ratio of Ag to AgCl was lower than 1 : 3, almost no pores could be observed.

3.2 The composition of hollow Ag/AgCl microcubes

The composition and surface chemical state of Ag/AgCl hollow microcubes can be investigated by EDS and XPS. In Fig. 4, EDS of the Ag/AgCl hollow microcubes exhibited strong peaks of Ag, Cl, and O. The ratios of Ag to AgCl are about 2.24 : 1, 0.8 : 1, 1 : 2.94 and 0 in EDS spectra corresponding to Ag/AgCl microcubes with various compositions (Ag : AgCl, (a) 3 : 1, (b) 1 : 1, (c) 1 : 3, and (d) 0 : 1). This variation in readings of actual content and observed amount is because the EDS technique takes into account a particular point instead of the whole catalyst surface for analysis, and thus, the metal concentration or percentage may be less than expected.[26] In these spectra, when the amount of $FeCl_3$ increases, the ratio of Cl to Ag equally increases, which indicates that more AgCl was generated in the obtained products. This result was consistent with that of XRD mentioned above. XPS spectra of Ag/AgCl hollow microcubes with various compositions are shown in Fig. 5. All binding energies were corrected by the reference value of C 1s (284.6 eV). In Fig. 5, the spectrum of Ag 3d with two peaks (367.0 and 373.0 eV) corresponded separately to the binding energies of Ag $3d_{5/2}$ and Ag $3d_{3/2}$.[30,31] In Fig. 5a, the peaks of Ag 3d deconvolution were respectively 373.5, 374.1, 367.5 and 368.4 eV. The peaks at 374.1 and 368.4 eV were attributed to the peak of metal Ag^0, while the bands at 373.5 and 367.5 eV could be attributed to the peak of Ag^+.[32] In Fig. 5a–c, there were Ag and AgCl in the Ag/AgCl products, but in Fig. 5d, no peak of metal Ag^0 was observed, which indicated that Ag has been totally transformed to AgCl. According to the area of fitting peaks, the molar ratios of Ag^0 to Ag^+ (3 : 1, 1 : 1, 1 : 3 and 0) could be calculated. With the

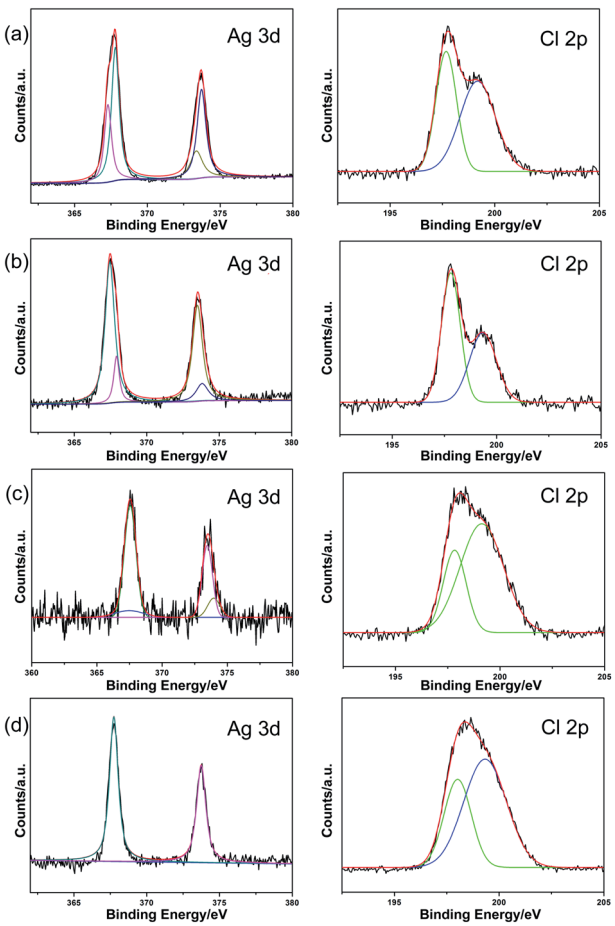

Fig. 5 XPS spectra of Ag/AgCl microcubes with various compositions (Ag : AgCl, (a) 3 : 1, (b) 1 : 1, (c) 1 : 3, and (d) 0 : 1).

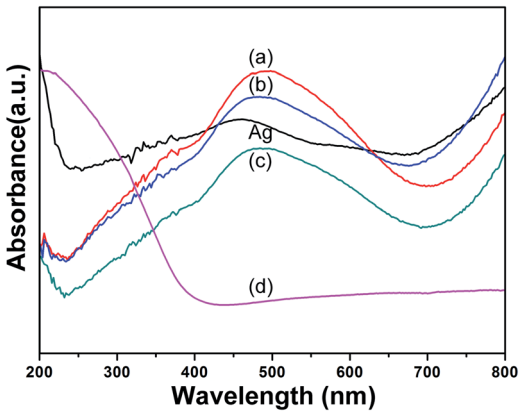

Fig. 6 UV-Vis absorption spectra of Ag/AgCl microcubes with various compositions (Ag : AgCl, (a) 3 : 1, (b) 1 : 1, (c) 1 : 3, and (d) 0 : 1).

increase of $FeCl_3$, the ratio of Ag^0 to AgCl decreased, clearly indicating that Ag^0 was oxidized to Ag^+. The Cl 2p spectrum in Fig. 5 corresponded to the binding energy of Cl $2p_{1/2}$ and Cl $2p_{3/2}$, respectively. Furthermore, EDS and XPS results suggested that Ag/AgCl hollow microcubes with controllable components could be obtained by this method.

3.3 Photocatalytic activity and mechanism

In addition, the UV-Vis absorption spectra of the products with different component ratios are shown in Fig. 6. In the spectra Fig. 6a–c, there was a wide absorption peak in the visible range of 400–700 nm owing to the several reflections inside the interior hollow structure, the increase of the average photon path length, and the surface plasmon resonance effect of Ag.[33] In Fig. 6d, the AgCl sample can absorb solar energy with wavelengths shorter than 400 nm and no absorption peak was observed in the visible range.[12]

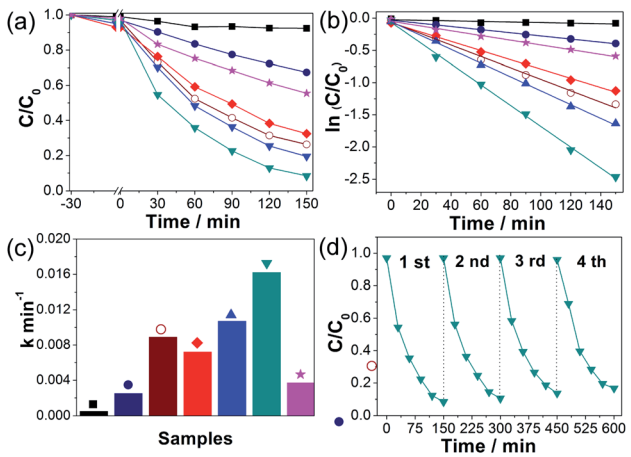

Fig. 7 (a) Photocatalytic degradation of phenol under visible light using various photocatalysts (■ blank experiment, ● N-TiO_2, ○ Ag/P25-TiO_2, hollow Ag/AgCl and Ag/AgCl microcubes) with various compositions (Ag : AgCl, ◆ 3 : 1, ▲1 : 1, ▼ 1 : 3 and ★ 0 : 1). (b) Linear kinetics for photodegradation of phenol by different photocatalysts, (c) kinetic constants, and (d) cycling degradation rate for phenol of Ag/AgCl (Ag : AgCl = 1 : 3).

To determine the photocatalytic performance of the synthesized Ag/AgCl hollow microcubes, we carried out photocatalytic phenol degradation experiments under visible light with the obtained products having different component ratios. For comparison, N-TiO_2 and P25-TiO_2/Ag were used as photocatalysts and their relative information is provided in Fig. S1.† Fig. 7 displays the time-dependent change of the ratio of phenol concentration to initial concentration measured according to the photocatalytic process. It could be seen from Fig. 7 that the photocatalytic activity of Ag/AgCl was the highest with the ratio of Ag to AgCl (1 : 3), and more than 91.6% of phenol could be degraded in 150 min. Fig. 7b can be characterized as the first-order rate constant diagram of phenol degradation by various products under visible light, and the illustration showed the degradation rate histogram. It can be seen from the figure that the first-order rate constants are 0.0005, 0.0025, 0.0089, 0.0072, 0.0107, 0.0162 and 0.0037 min^{-1}, corresponding to the blank experiment (without a catalyst), N-TiO_2, Ag/P25-TiO_2, Ag/AgCl with various compositions (the ratio of Ag to AgCl: 3 : 1, 1 : 1, and 1 : 3) and pure AgCl, respectively. The maximum rate constant of AgCl/Ag (the ratio of Ag to AgCl = 1 : 3) was about 6.48-fold and 1.82-fold higher than that of N-TiO_2 and Ag/P25-TiO_2 nanoparticles.

For the good application of a photocatalyst, its stability is as important as its photocatalytic activity. Therefore, the stability of the photocatalyst with the Ag/AgCl ratio of 1 : 3 was studied by cyclic experiments. As shown in Fig. 7d, even after four cycling runs of phenol photodegradation, the photocatalytic activity has no obvious change, which indicates that the prepared Ag/AgCl hollow microcube photocatalyst has good photocatalytic stability.

The photocatalysis mechanism of Ag/AgCl hollow microcubes was disclosed by active species trapping measurements. In this work, isopropyl alcohol (IPA), benzoquinone (BQ) and triethanolamine (TEOA) were applied to scavenge $^{\bullet}OH$, $^{\bullet}O_2^-$ and h^+, respectively.[34,35] It was found that no obvious decrease of photocatalytic performance was observed when IPA was added, indicating that $^{\bullet}OH$ could not change the photocatalytic process. Nevertheless, the degradation efficiencies decreased greatly with the existence of benzoquinone (BQ) and triethanolamine (TEOA), confirming that the main active species were $^{\bullet}O_2^-$ and h^+ and played an important role in the process of photocatalysis.

According to the above active species trapping measurement results, a possible photocatalytic mechanism of Ag/AgCl was proposed and is shown in Fig. 8. It is reported that the band gap of AgCl is about 3.25 eV.[36,37] Based on UV-Vis reflectance spectrometry in Fig. 6, the band gap of AgCl can be determined by the following equation:[38]

$$\alpha h\nu = A\left(h\nu - E_g\right)^{\frac{n}{2}}$$

where α, ν, E_g and A are the absorption coefficient, light frequency, band gap, and a constant, respectively. For AgCl, the value of n is 4 for the indirect transition[39] and the intercept of the tangent to the X axis would give a good approximation of the E_g (Fig. S2†). The band gap of the AgCl sample obtained is about

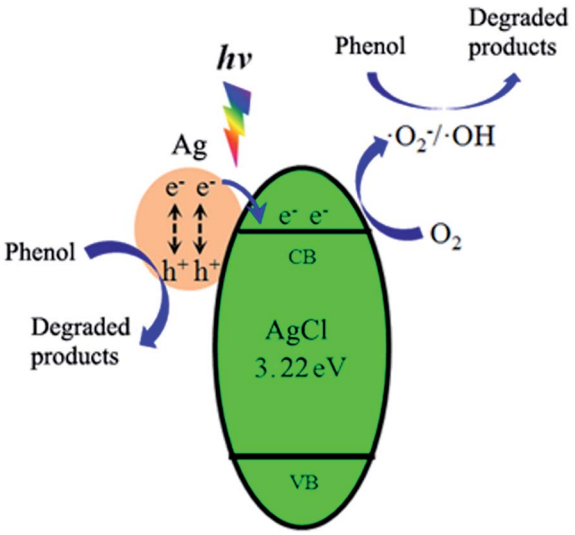

Fig. 8 The proposed schematic diagram of the Ag/AgCl composite for the photocatalytic degradation of phenol under visible light irradiation.

3.22 eV, which is close to the value in the literature.[36,37] Clearly, AgCl can't absorb visible light owing to its wide band gap. Therefore, the photo-produced electrons were only generated by Ag nanoparticles due to the SPR effect. The generated hot electrons of Ag nanoparticles under visible light have sufficient energy within 1.0–4.0 eV and the electrons could be transferred to the conduction band of AgCl.[5,11] As the conduction band potential of AgCl (−0.06 eV) is more negative than that of O_2/$^{\bullet}O_2^-$ (−0.046 eV), the oxygen dissolved in the solution captured the electrons on the surface of AgCl to produce $^{\bullet}O_2^-$ active species, which can further oxidize the phenol.[40] Meanwhile, the remaining photoinduced holes of Ag nanoparticles could also directly contribute to oxidize phenol. The compact interface of Ag/AgCl hollow microcubes could effectively promote the photoelectron transfer and yield the improvement of photocatalytic performance.

The mechanism proposed could also be used to explain the dependence of photocatalytic performance on the ratio of Ag to AgCl in our experiment of photocatalytic degradation of phenol. According to the mechanism, photocatalytic performance of Ag/AgCl hollow microcubes was related to the hot electron concentration of Ag and the separation efficiency of photoinduced carriers was dependent on the amount of Ag nanoparticles in Ag/AgCl and on the nanoscale spatial distribution of supported Ag nanoparticles.[21,22] Based on the experimental results of photocatalytic degradation of phenol, the as-obtained Ag/AgCl hollow microcubes (the ratio of Ag to AgCl = 1 : 3) showed the highest photocatalytic capability under visible-light illumination. The reason might be ascribed to two aspects including the content of Ag and the surface porous structure of Ag/AgCl hollow microcubes in our experiments. Ag/AgCl hollow microcubes (the ratio of Ag to AgCl = 3 : 1) not only have the most visible light absorbance but also more number of pores on the surface which results in higher adsorption capability for phenol molecules than all other Ag/AgCl. However, it still exhibited lower photocatalytic performance than the Ag/AgCl hollow microcubes (the ratio of Ag to AgCl = 1 : 1 and 1 : 3), which may be related to the content of Ag in the Ag/AgCl composite microcubes, since photocatalytic performance was also strongly influenced by the content of Ag in previously reported composite catalysts.[33,41] For the as-obtained Ag/AgCl composite microcubes, Ag nanoparticles would produce photogenerated hot electrons and holes under visible light illumination, which can be transferred to the conduction band of AgCl.[9,12] Consequently, the photocatalytic performance of the AgCl/Ag samples depends intimately on the interaction between AgCl and metallic Ag. It was reported that the interface between the AgCl and Ag would be enlarged with the higher Ag content in the Ag/AgCl composite, thereby increasing hole capture by the negative surface charge on the Ag nanoparticles, which may reduce the efficiency of charge separation.[42] In addition, high proportion of Ag in Ag/AgCl hollow microcubes enhances electron capture by neighboring Ag nanoparticles and reduces the photocatalytic activity.[21] In a word, the proper content of Ag and surface structure of Ag/AgCl microcubes in our experiments made the Ag/AgCl (the ratio of Ag to AgCl = 1 : 3) show the highest photocatalytic activities.

4. Conclusions

In summary, Ag/AgCl hollow microcube photocatalysts with different components and a number of tiny Ag/AgCl heterojunctions were successfully synthesized by the oxidation of a nanosheet-assembled Ag hollow microcube template. By adjusting the quantity of the oxidizing agent $FeCl_3$, the microcubes with various compositions were obtained. The Ag/AgCl hollow microcubes with adjustable compositions could not only result in multiple light reflections in the cavity with an improvement in the visible light absorption ability, but also enhance the separation efficiency of photogenerated charges by regulating the heterojunction interface of Ag/AgCl. Ag/AgCl hollow microcubes with a ratio of Ag to AgCl of 1 : 3 had the best photocatalytic performance for the degradation of 91.6% of phenol in 150 min, which was mainly ascribed to the efficient light-harvesting for the generation of photoinduced carriers in Ag/AgCl and effective charge separation at the interfaces between Ag and AgCl. This study provides a new possibility for the rational design of other highly efficient composite photocatalysts through structural and component regulation.

Author contributions

Shiyun Lou: conceptualization, investigation, and writing original draft. Qinglan Chen: investigation, formal analysis, and validation. Wan Wang: investigation and data curation. Yongqiang Wang: investigation. Shaomin Zhou: conceptualization, supervision, and project administration.

Conflicts of interest

There are no conflicts to declare.

Acknowledgements

This work was supported by the National Natural Science Foundation of China (No. 51372070 and No. 21371049), Fundamental and Frontier Research Project of Henan Province, China (No. 162300410040), the Key Project of Education Department of Henan Province, China (No. 14B430010), and the Key Scientific and Technological Research Project of Henan Province, China (202102310598).

References

1 X. Y. Zhang, Y. N. Chen, Q. K. Shang and Y. N. Guo, Copper doping and organic sensitization enhance photocatalytic activity of titanium dioxide: Efficient degradation of phenol and tetrabromobisphenol A, *Sci. Total Environ.*, 2020, **716**, 137144.

2 T. Ahmad, J. Iqbal, M. A. Bustam, M. Zulfiqar, N. Muhammad, B. M. Al Hajeri, M. Irfan, H. M. A. Asghar and S. Ullah, Phytosynthesis of cerium oxide nanoparticles and investigation of their photocatalytic potential for degradation of phenol under visible light, *J. Mol. Struct.*, 2020, **1217**, 128292.

3 M. C. N. Martinez, B. Bajorowicz, T. Klimczuk, A. Zak, J. Luczak, W. Lisowski and A. Zaleska-Medynska, Synergy between $AgInS_2$ quantum dots and ZnO nanopyramids for photocatalytic hydrogen evolution and phenol degradation, *J. Hazard. Mater.*, 2020, **398**, 123250.

4 S. W. Li, P. Miao, Y. Y. Zhang, J. Wu, B. Zhang, Y. C. Du, X. J. Han, J. M. Sun and P. Xu, Recent advances in plasmonic nanostructures for enhanced photocatalysis and electrocatalysis, *Adv. Mater.*, 2020, **33**(6), 2000086.

5 Z. Z. Lou, S. Kim, M. Fujitsuka, X. G. Yang, B. J. Li and T. Majima, Anisotropic Ag_2S-Au triangular nanoprisms with desired configuration for plasmonic photocatalytic hydrogen generation in visible/near-infrared region, *Adv. Funct. Mater.*, 2018, **28**(13), 1706969.

6 N. Q. Wu, Plasmonic metal-semiconductor photocatalysts and photoelectrochemical cells: a review, *Nanoscale*, 2018, **10**(6), 2679–2696.

7 M. Norouzi, A. Fazeli and O. Tavakoli, Phenol contaminated water treatment by photocatalytic degradation on electrospun Ag/TiO_2 nanofibers: Optimization by the response surface method, *J. Water Process. Eng.*, 2020, **37**, 101489.

8 A. Shet and K. V. Shetty, Solar light mediated photocatalytic degradation of phenol using Ag core-TiO_2 shell (Ag@TiO_2) nanoparticles in batch and fluidized bed reactor, *Sol. Energy*, 2016, **127**, 67–78.

9 C. H. An, S. Peng and Y. G. Sun, Facile synthesis of sunlight-driven AgCl:Ag plasmonic nanophotocatalyst, *Adv. Mater.*, 2010, **22**(23), 2570–2574.

10 Y. P. Bi and J. H. Ye, In situ oxidation synthesis of Ag/AgCl core-shell nanowires and their photocatalytic properties, *Chem. Commun.*, 2009, **43**, 6551–6553.

11 Y. X. Tang, Z. L. Jiang, G. C. Xing, A. R. Li, P. D. Kanhere, Y. Y. Zhang, T. C. Sum, S. Z. Li, X. D. Chen, Z. L. Dong and Z. Chen, Efficient Ag@AgCl cubic cage photocatalysts profit from ultrafast plasmon-induced electron transfer processes, *Adv. Funct. Mater.*, 2013, **23**(23), 2932–2940.

12 P. Wang, B. B. Huang, X. Y. Qin, X. Y. Zhang, Y. Dai, J. Y. Wei and M. H. Whangbo, Ag@AgCl: A highly efficient and stable photocatalyst active under visible light, *Angew. Chem., Int. Ed.*, 2008, **47**(41), 7931–7933.

13 B. Ma, J. Guo, W. Da and K. Fan, Highly stable and efficient Ag/AgCl core–shell sphere: Controllable synthesis, characterization, and photocatalytic application, *Appl. Catal., B*, 2013, **130**, 257–263.

14 M. J. Guo, Z. P. Xing, T. Y. Zhao, Y. L. Qiu, B. Tao, Z. Z. Li and W. Zhou, Hollow flower-like polyhedral alpha-Fe_2O_3/Defective MoS_2/Ag Z-scheme heterojunctions with enhanced photocatalytic-fenton performance *via* surface plasmon resonance and photothermal effects, *Appl. Catal., B*, 2010, **272**, 118978.

15 J. Richard-Daniel and D. Boudreau, Enhancing galvanic replacement in plasmonic hollow nanoparticles: Understanding the role of the speciation of metal ion precursors, *ChemNanoMat*, 2020, **6**(6), 907–915.

16 A. Genc, J. Patarroyo, J. Sancho-Parramon, N. G. Bastus, V. Puntes and J. Arbiol, Hollow metal nanostructures for enhanced plasmonics: synthesis, local plasmonic properties and applications, *Nanophotonics*, 2017, **6**(1), 193–213.

17 M. Nazemi and M. A. El-Sayed, Plasmon-enhanced photo(electro)chemical nitrogen fixation under ambient conditions using visible light responsive hybrid hollow Au-Ag_2O nanocages, *Nano Energy*, 2019, **63**, 103886.

18 J. Feng and Y. D. Yin, Self-templating approaches to hollow nanostructures, *Adv. Mater.*, 2019, **31**(38), 1802349.

19 P. Wang, B. B. Huang, Z. Z. Lou, X. Y. Zhang, X. Y. Qin, Y. Dai, Z. K. Zheng and X. N. Wang, Synthesis of highly efficient Ag@AgCl plasmonic photocatalysts with various structures, *Chem.–Eur. J.*, 2009, **16**(2), 538–544.

20 S. K. Wu, X. P. Shen, Z. Y. Ji, G. X. Zhu, C. J. Chen, K. M. Chen, R. Bu and L. M. Yang, Synthesis of AgCl hollow cubes and their application in photocatalytic degradation of organic pollutants, *CrystEngComm*, 2015, **17**(12), 2517–2522.

21 T. Yoshida, Y. Misu, M. Yamamoto, T. Tanabe, J. Kumagai, S. Ogawa and S. Yagi, Effects of the amount of Au nanoparticles on the visible light response of TiO_2 photocatalysts, *Catal. Today*, 2020, **352**, 34–38.

22 A. Holm, E. D. Goodman, J. H. Stenlid, A. Aitbekova, R. Zelaya, B. T. Diroll, A. C. Johnston-Peck, K.-C. Kao, C. W. Frank, L. G. M. Pettersson and M. Cargnello, Nanoscale spatial distribution of supported nanoparticles controls activity and stability in powder catalysts for CO oxidation and photocatalytic H_2 evolution, *J. Am. Chem. Soc.*, 2020, **142**(34), 14481–14494.

23 Y. P. Bi and J. H. Ye, Direct conversion of commercial silver foils into high aspect ratio AgBr nanowires with enhanced photocatalytic properties, *Chem.–Eur. J.*, 2010, **16**(34), 10327–10331.

24 S. Y. Lou, W. Wang, L. X. Wang and S. M. Zhou, In-situ oxidation synthesis of Cu_2O/Ag/AgCl microcubes with enhanced visible-light photocatalytic activity, *J. Alloys Compd.*, 2019, **781**, 508–514.

25 Y. Q. Wang, T. Gao, K. Wang, X. P. Wu, X. J. Shi, Y. B. Liu, S. Y. Lou and S. M. Zhou, Template-assisted synthesis of uniform nanosheet-assembled silver hollow microcubes, *Nanoscale*, 2012, **4**(22), 7121–7126.

26 M. K. Aulakh, R. Sharma, B. Pal and R. Prakash, Photo-induced oxidation and reduction by plasmonic Ag-TiO_2 nanocomposites under UV/sunlight, *Sol. Energy*, 2020, **196**, 427–436.

27 A. A. Melvin, K. Illath, T. Das, T. Raja, S. Bhattacharyya and C. S. Gopinath, M-Au/TiO_2 (M = Ag, Pd, and Pt) nanophotocatalyst for overall solar water splitting: role of interfaces, *Nanoscale*, 2015, **7**(32), 13477–13488.

28 X. L. Yan, T. Ohno, K. Nishijima, R. Abe and B. Ohtani, Is methylene blue an appropriate substrate for a photocatalytic activity test? A study with visible-light responsive titania, *Chem. Phys. Lett.*, 2006, **429**(4–6), 606–610.

29 F. Hayati, A. A. Isari, M. Fattahi, B. Anvaripour and S. Jorfi, Photocatalytic decontamination of phenol and petrochemical wastewater through ZnO/TiO_2 decorated on reduced graphene oxide nanocomposite: influential operating factors, mechanism, and electrical energy consumption, *RSC Adv.*, 2018, **8**(70), 40035.

30 X. J. Wen, C. G. Niu, D. W. Huang, L. Zhang, C. Liang and G. M. Zeng, Study of the photocatalytic degradation pathway of norfloxacin and mineralization activity using a novel ternary Ag/AgCl-CeO_2 photocatalyst, *J. Catal.*, 2017, **355**, 73–86.

31 S. Y. Lou, X. B. Jia, Y. Q. Wang and S. M. Zhou, Template-assisted *in situ* synthesis of porous AgBr/Ag composite microspheres as highly efficient visible-light photocatalyst, *Appl. Catal., B*, 2015, **176**, 586–593.

32 N. N. Wang, K. Cheng, Z. F. Xu, P. Li, G. W. Geng, C. C. Chen, D. J. Wang, P. L. Chen and M. H. Liu, High-performance natural-sunlight-driven Ag/AgCl photocatalysts with a cube-like morphology and blunt edges *via* a bola-type surfactant-assisted synthesis, *Phys. Chem. Chem. Phys.*, 2020, **22**(7), 3940–3952.

33 H. Y. Li, T. S. Wu, B. Cai, W. G. Ma, Y. J. Sun, S. Y. Gan, D. X. Han and L. Niu, Efficiently photocatalytic reduction of carcinogenic contaminant Cr(VI) upon robust AgCl:Ag hollow nanocrystals, *Appl. Catal., B*, 2015, **164**, 344–351.

34 S. F. Yang, C. G. Niu, D. W. Huang, H. Zhang, C. Lianga and G. M. Zeng, $SrTiO_3$ nanocubes decorated with Ag/AgCl nanoparticles as photocatalysts with enhanced visible-light photocatalytic activity towards the degradation of dyes, phenol and bisphenol A, *Environ. Sci.: Nano*, 2017, **4**(3), 585–595.

35 Y. X. Yang, W. Guo, Y. N. Guo, Y. H. Zhao, X. Yuan and Y. H. Guo, Fabrication of Z-scheme plasmonic photocatalyst Ag@AgBr/g-C_3N_4 with enhanced visible-light photocatalytic activity, *J. Hazard. Mater.*, 2014, **271**, 150–159.

36 Z. K. Xu, L. Han, P. Hu and S. J. Dong, Facile synthesis of small Ag@AgCl nanoparticles *via* a vapor diffusion strategy and their highly efficient visible-light-driven photocatalytic performance, *Catal. Sci. Technol.*, 2014, **4**(10), 3615–3619.

37 J. Tejeda, N. J. Shevchik, W. Braun, A. Goldmann and M. Cardona, Valence bands of AgCl and AgBr: UV photoemission and theory, *Phys. Rev. B*, 1975, **12**, 1557–1566.

38 X. Zhang, L. Z. Zhang, T. F. Xie and D. J. Wang, Low-temperature synthesis and high visible-light-induced photocatalytic activity of BiOI/TiO_2 heterostructures, *J. Phys. Chem. C*, 2009, **113**(17), 7371–7378.

39 P. K. de Boer and R. A. de Groot, Conduction band of the photographic compound AgCl, *J. Phys. Chem. A*, 1999, **103**, 5113–5115.

40 J. He, D. W. Shao, L. C. Zheng, L. J. Zheng, D. Q. Feng, J. P. Xu, X. H. Zhang, W. C. Wang, W. H. Wang, F. Lu, H. Dong, Y. H. Cheng, H. Liu and R. K. Zheng, Construction of Z-scheme Cu_2O/Cu/AgBr/Ag photocatalyst with enhanced photocatalytic activity and stability under visible light, *Appl. Catal., B*, 2017, **203**, 917–926.

41 M. S. Zhu, P. L. Chen and M. H. Liu, Ag/AgBr/graphene oxide nanocomposite synthesized *via* oil/water and water/oil microemulsions: A comparison of sunlight energized plasmonic photocatalytic activity, *Langmuir*, 2012, **28**(7), 3385–3390.

42 J. Jiang and L. Zhang, Rapid microwave-assisted nonaqueous synthesis and growth mechanism of AgCl/Ag, and its daylight-driven plasmonic photocatalysis, *Chem.–Eur. J.*, 2011, **17**(13), 3710–3717.